

Thoracic Organ Segmentation using U-Net Deep Learning Architecture

Will Argus
wargus@eng.ucsd.edu

Harmeet Gill
hsgill@eng.ucsd.edu

Karndeeep Singh
kraibhat@eng.ucsd.edu

Abstract— In this paper, we will discuss our implementation of deep learning to segment organs in CT scans of the human thorax. The dataset, and methods are provided by a competition hosted during the Annual Meeting of American Association of Physicists in Medicine in 2017.

Keywords—AAPM, Dice, U-Net, DICOM, Thoracic, Binary Cross entropy

I. INTRODUCTION

In 2017, the Annual Meeting of American Association of Physicists in Medicine (AAPM) hosted a challenge intended to encourage exploration and evaluation of machine learning approaches for auto-segmenting Computed tomography (CT) scans. In medicine, CT scans are used to map the internal anatomy of the body based on x-ray attenuation measurements. These measurements are made at different angles around the body and used to reconstruct cross sectional images.

Even if a CT scan can be used to visualize the organs within a body, more work is required to make the CT scan useful. In the case of radiation therapy, a common use case for CT scans, the location of the entire organ of interest must be identified and annotated on a CT scan in a process called segmentation. Typically this is done manually, a tedious process where a radiologist combs through the entire volume of images marks each pixel that shows the organ of interest. The idea behind auto-segmentation is that this process can be automated such that it is faster, cheaper, and gives more consistent results.

Returning to the topic of the 2017 annual meeting of the AAPM, all groups were given the same dataset and graded using the same criteria. The designated organs of interest were the heart, spinal cord, esophagus, and the right and left lungs. This paper will detail the authors' implementation of one of the approaches involving a U-Net using the same dataset used in the competition

II. RELATED WORK

This problem was approached by a group in the University of South Carolina, which trained a deep CNN to segment the CT scans using specific orthogonal 2D slices of the scans. The CNN used coarse feature recognition and then fine extraction to segment the pixels of the 3D scans. This solution focused on real time segmentation. They segmented 2 organs,

the left kidney and the pancreases, with an intersection over union score of 88 and 65 percent accuracy, respectively.

The general CNN architecture used by the competition team whose approach the authors are implementing here, is known as a U-Net and was developed by a group at the University of Freiburg, Germany. The U-Net architecture is common in biomedical image processing due to its ability to assign a label to each pixel in an image, meaning that it can identify specific desired regions in an image.

III. DATASET AND FEATURES

Our data set was put together by the AAMP to serve as a benchmark for comparing Auto-Segmentation methods. The Dataset consists of 60 thoracic CT scans. All cross sectional images are 512 by 512 pixels. The height of a given volume varies, but is on average 130 images. Images were taken using 3 different scanners at different institutes (20 scans each). This leads to significant variation between volumes. These variations are both due to differences in patients (body fat, bone structure), as well as scanner settings (slice thickness, scanner voltage, scanner quality). CT data was presented in the native dicom format.

Each CT volume was accompanied by a segmentation file. Volumes were manually and independently annotated by 3 radiologists following guidelines. The provided segmentations were generated via pairwise comparison of the radiologists' annotations. Every included the following labeled and non-overlapping regions: Heart, Esophagus, Spinal Cord, and Lungs.

For this task, the features that we hope to detect are well defined. We wanted to identify organs, each with its own set of defining features. For example, the spinal cord can be recognized by its shape as well as the sharp change in attenuation coefficients from the bone to tissue. The Lungs similarly benefit, mainly being filled with air and being surrounded by tissue.

IV. METHODS AND MODEL

A. U-Net Architecture

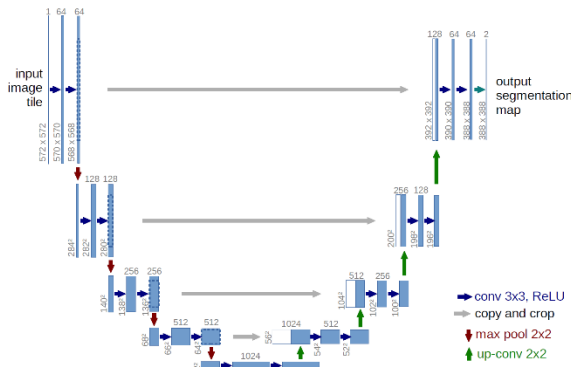


Figure 1 - Diagram of U-net architecture published by the Brox research group

The U-Net is a Convolutional Network designed specifically for biomedical image segmentation. An image is input into the network. The network outputs a binary mask corresponding to the region of interest.

The network architecture resembles that of an autoencoder, consisting of a contracting path, a bottleneck, and an expanding path. The contracting path consists of a single unit repeated 4 times. The unit consists of a convolutional layer followed by a ReLU activation layer repeated twice, followed by a max pooling layer. The bottleneck consists of two more convolutional layers with ReLU activations functions. The expansive layer consists of an analogous unit to the contracting path being repeated 4 times. This consists of upsampling followed by a 2x2 convolutional layer and the same convolutional layers with ReLU activations.

Prior to every maxpool layer in the contracting path, a skip connection connects the layer to the corresponding layer in the expanding path. These skip connections serve to ensure the robust maintenance of spatial information within the network. The final layer consisted of a sigmoid function. This is coupled to a binary cross entropy loss. In training, the Adam optimizer was used.

$$\text{Binary CrossEntropy} = \sum_{i=0} y_{i,pred} \log(y_{i,truth})$$

Due to the kernel size used for each of the 23 convolutional layers, the model is only able to accurately predict information in the central two thirds of the image. This is due to a loss of information at the edges of the matrix with every convolution.

B. Our Model Specifics

Dropout layers were included within the model to reduce over fitting with the goal of improving the generalization of the model. One dropout layer was included at the end of the contracting path and another following the bottleneck. This specific configuration was chosen to optimize the compact representation at the end of the bottleneck. No earlier dropouts were included to maintain the integrity of the high level spatial information used in reconstruction. Similarly, no dropouts were included in the expansive (generative) path.

Within the dataset, positively labeled voxels for several of the target labels suffered from class imbalance. For example, the heart made up approximately 1% of the pixels in a CT volume. The approach taken in our study was to segment every organ individually, further exacerbating the problem of class imbalance.

To solve this, the dataset was resampled. All slices containing any positive label were separated out. Along with this, a set number of slices were randomly selected from the rest of the volume to represent the remainder of the images. The model was then trained on this subset.

This solution was only applicable to the heart. Organs such as the spine and esophagus with very small segmented areas in a majority of slices. Accounting for this would require implementing alternative loss functions.

V. EXPERIMENTS, RESULTS AND DISCUSSION

Results of the model varied between the four organs. A separate but identical neural network was used for each of the organ segmentations, with 36 CT volumes for training, 9 for validation and 15 for testing. During the training process, CT volumes were broken down by individual slices, and passed to the training model via a generator function by a batch size of 5 stacks (5x512x512x1 array density). Each epoch stepped through all the training images for all volumes, thus a large number of epochs were not necessary before the model started to over fit.

The Dice coefficient was used to judge performance of the model. This metric divides the union between truth and prediction with the total sum of both objects, and gives a better indication of whether our prediction remained in the same space as the ground truth.

$$\text{Dice} = \frac{2|y_{truth} \cup y_{pred}|}{|y_{truth}| + |y_{pred}|}$$

A summary of the Dice scores for each organ can be found in Table 1.

A. Heart

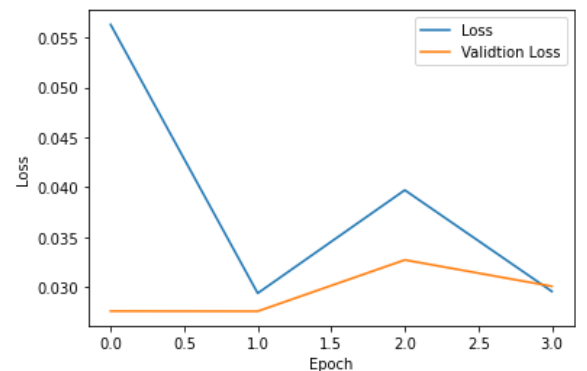


Figure 2 - Binary Cross-Entropy loss of heart training for 4 epochs

Our heart region was well predicted, with a loss of less than 3.5 percent. The loss function in any instance was calculated using the images in a single batch, therefore does not

necessarily indicate a fully stacked volumetric loss value. Because of this, low loss models were still observed to have volumetric inconsistency as seen in the stacked dimension. This can be seen in Figure 3, where the top of the heart prediction in the right object has discontinuous slices, while the left ground truth is consistent.

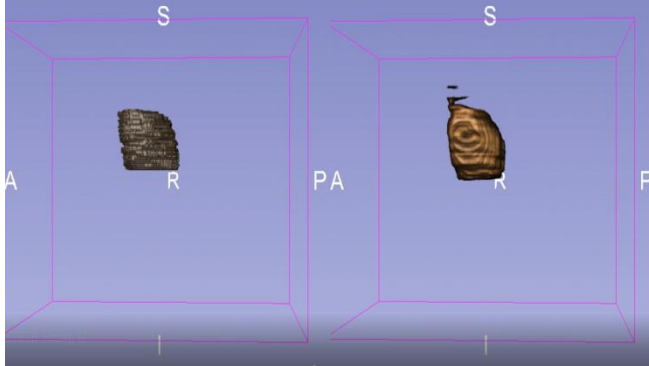


Figure 3 - 3-D view of heart with ground truth on left, and prediction on right

One problem that was prevalent in heart training was class imbalance. Initially, most of the training images were void of any true pixel labels. As a result, our model did not predict the heart region well after training. To mitigate this, the training files were split into sections that contained true labels and sections that did not. All sections that contained true labels were fed into the model, and an equally volumetric stack containing randomized selection of sparse images were also fed in.

B. Esophagus

The esophagus, of all the organ predictions, was the worst predicted. Figure 4 shows the binary-cross entropy loss of the esophagus training for 6 epochs. Although the training and validation loss was low (approximately 0), this is not indicative of the accuracy of the model with respect to the segmented masks. Because the esophagus occupies a small region at any given slice (as can be seen in Figure 5), the majority of weight in the loss calculation is being done on pixels with a value of zero, which is skewing the value down. A more sensitive measurement of volumetric similarity can be achieved using the dice coefficient. Our mean Dice coefficient against 15 test volumes was 8.8 percent, which is indicative of a bad fit.

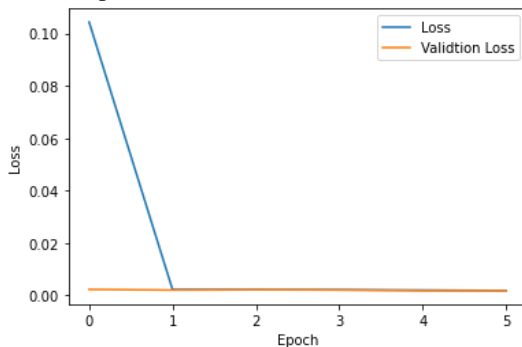


Figure 4 - Binary Cross-Entropy loss of esophagus training for 6 epochs

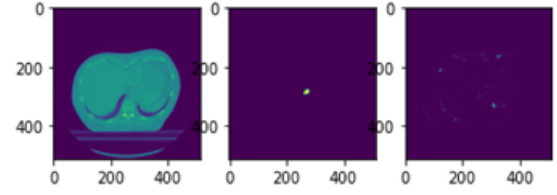


Figure 5 - Slice comparison of esophagus, left image is raw CT scan, middle image indicated binary mask, and right image indicated the neural net prediction

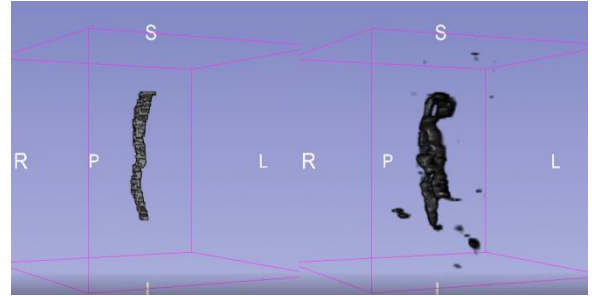


Figure 6 - 3-D view of esophagus with ground truth on left, and prediction on right

B. Spinal Cord

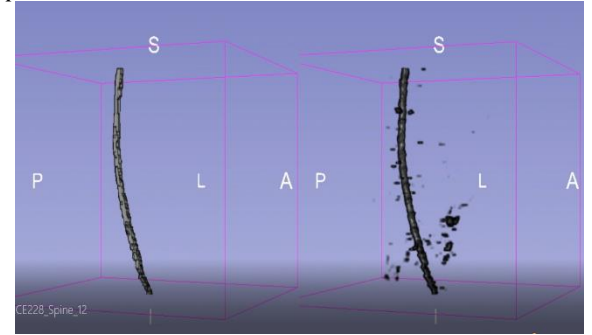


Figure 7 - 3-D view of spine with ground truth on left, and prediction on right

The spine prediction, although noisy in the sparse regions, predicted the volume and shape of the binary CT stack very well. As seen in Figure 7, the curvature and volumetric consistency was tracked well over the stacks. Figure 8 shows the loss function over 4 epochs, with an end loss of less than 1 percent for both the training and validation set. The average spine Dice coefficient was 75.5 percent, which indicates the model intelligently predicting the spine, but with some false positives in each stack. It's worth noting that with some thresholding of the predicted stack, much of this noise can potentially be taken out. The currently produced results have no post-processing applied.

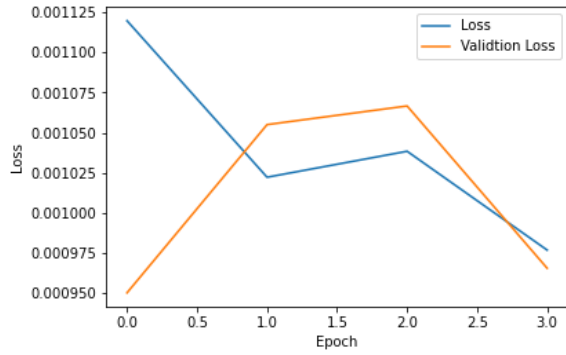


Figure 8 - Binary Cross-Entropy loss of spine training for 4 epochs

One interesting results produced by the spine can be seen in Figure 9. Because the 2017 competition only cared about segmenting the thoracic region, the spine segmentation stopped after reaching the neck area. Our model, however, was able to understand that the spine continued and kept predicting the correct spinal region into the neck. This obviously brought down the Dice score, but was a good indication of intelligent predicting.

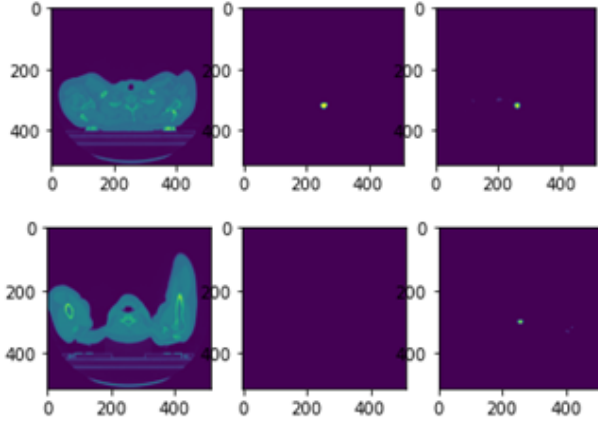


Figure 9 - Slice comparison of spine. left image is raw CT scan, middle image indicated binary mask, and right image indicated the neural net prediction. Above three images are showing the model correctly predicting spine, and below 3 images show our model prediction

C. Lungs

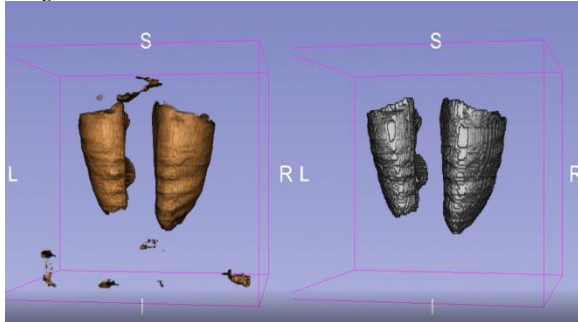


Figure 10 - 3-D view of spine with ground truth on left, and prediction on right

The lungs were well predicted with a loss of less than 5 percent. Similar issues with regard to volumetric noise can be seen in Figure 10, but otherwise the general shape and space was predicted well.

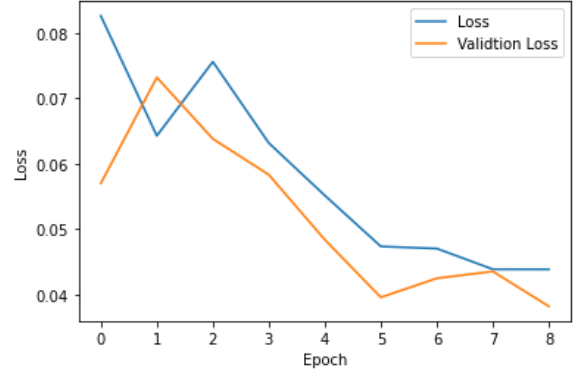


Figure 11 - Binary Cross-Entropy loss of lung training for 9 epochs

Table 1 - Dice Comparison of Results versus Paper [1]

	Dice (%) - Paper	Dice (%) - Results
Lung	95.2 +/- 5.6	95.6 +/- 1.9
Heart	89.3 +/- 9.5	93.1 +/- 1.5
Spine	75.5 +/- 7.3	86.2 +/- 3.8
Esophagus	8.8 +/- 11.4	81.8 +/- 3.9

VI. CONSLUSION

In conclusion, we were able to produce similar results to those in the AAPM competition for 3 of the 4 organs. It should be noted, that due to limited computational resources, our code had to be adjusted accordingly.

For future experiments, we would like to try consolidating all the binary masks and using one neural network model that outputs a one-hot-encoded results with a channel for each organ. This would work to address the problem of class imbalance and would also attribute the sparse space that is otherwise treated homogeneously to other organs. Additionally, we would like to test with other loss models as well as number of epochs to improve our results.

ACKNOWLEDGMENT

A. Will Argus

Contributed to the literature search as a well as data visualization, helped define some of the methods used in the final model.

B. Harmeet Gill

Helped with code prototyping and testing different functions and data processing. Contributed in label generating code and final

result generation.

C. Karandeep Singh

Created most of the final code after consolidating the coding and model experiments, and contributed to all other aspects of the project as well.

REFERENCES

- [1] Yang, J., Veeraraghavan, H., Armato, S. G., Farahani, K., Kirby, J. S., Kalpathy-Kramer, J., ... Sharp, G. C. (2018). *Auto-segmentation for Thoracic Radiation Treatment Planning: A Grand Challenge at AAPM 2017. Medical Physics*. doi:10.1002/mp.13141
- [2] Ronneberger, Olaf, et al. "U-Net: Convolutional Networks for Biomedical Image Segmentation." *Lecture Notes in Computer Science Medical Image Computing and Computer-Assisted Intervention – MICCAI 2015*, 2015, pp. 234–241., doi:10.1007/978-3-319-24574-4_28.
- [3] Çiçek, Özgün, et al. "3D U-Net: Learning Dense Volumetric Segmentation from Sparse Annotation." *Medical Image Computing and Computer-Assisted Intervention – MICCAI 2016 Lecture Notes in Computer Science*, 2016, pp. 424–432., doi:10.1007/978-3-319-46723-8_49.
- [4] Zhou, Xiangrong, et al. "Automated segmentation of 3D anatomical structures on CT images by using a deep convolutional network based on end-to-end learning approach." *Department of Computer Science and Engineering, University of South Carolina – Song Wang*, 2016